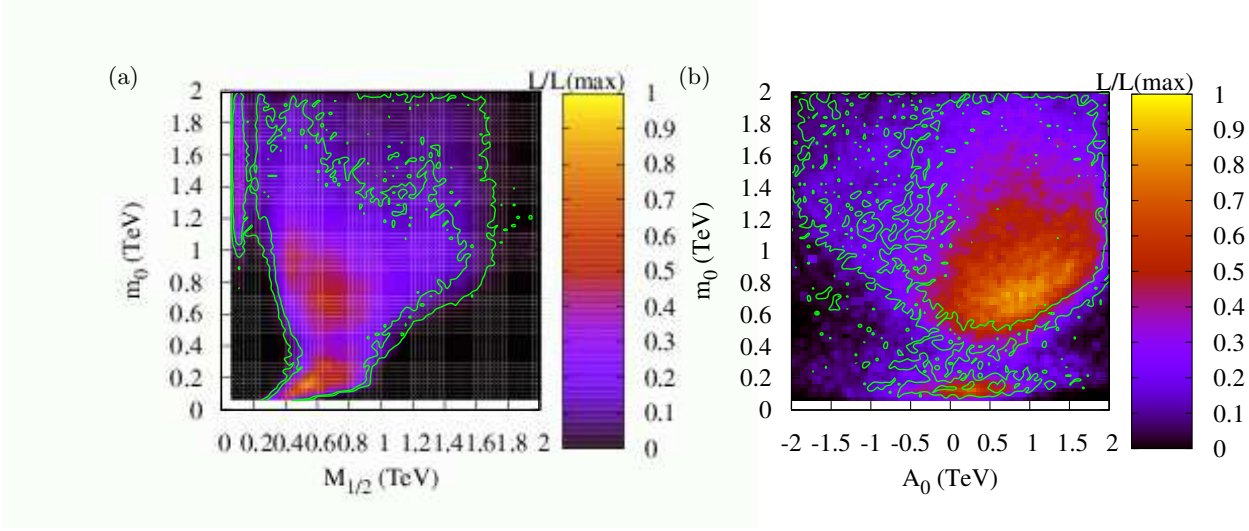

FIG. 6: Likelihood maps of mSUGRA parameter space including theoretical uncertainty. The graphs show the likelihood distributions sampled from 8d parameter space and marginalised down to two. The likelihood (relative to the likelihood in the highest bin) is displayed by reference to the bar on the right hand side of each plot.

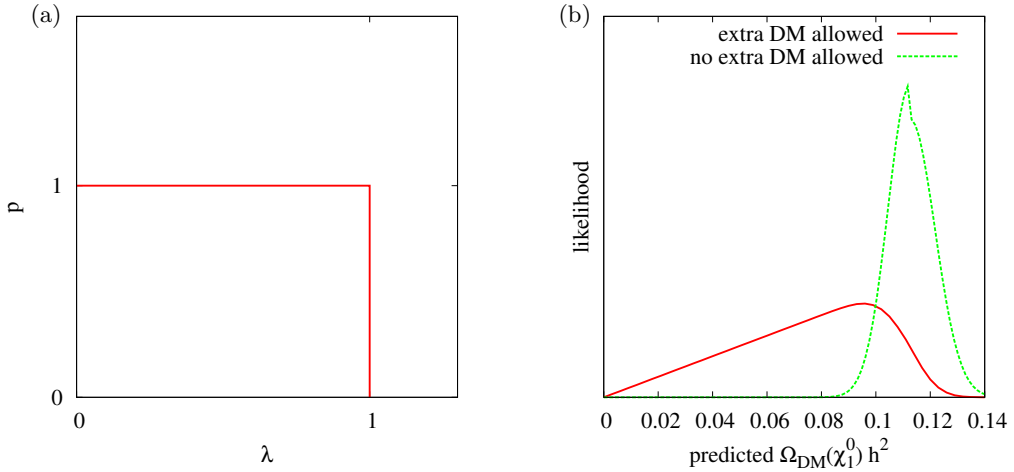

FIG. 7: (a) $p(\lambda|m_{\Omega_{DM}h^2})$, the probability distribution assumed for λ, the ratio of predicted SUSY dark matter to total dark matter, given some measured value $m_{\Omega_{DM}h^2}$. (b) Comparison of the likelihood penalty $\mathcal{L}_{\Omega_{DM}h^2}$ paid for a prediction of SUSY dark matter $p_{\Omega_{DM}h^2}$ with ("extra DM allowed") and without ("no extra DM allowed") the allowance of non thermal-neutralino dark matter.

the increased efficiency. Likelihoods of sparticle masses also look the same, except for the spike in the gluino mass, which has twice as much likelihood. As mentioned before, this spike is due mainly to the light h^0-pole region which is subject to relatively large fluctuations, as Tables IV,VI illustrate. We cannot conclude that the h^0-pole region obtains more integrated likelihood by admitting non thermal-neutralino components to the relic density because the statistics in the MCMC algorithm are not high enough.

One distribution that does significantly change shape is that of $BR(B_s \to \mu^+\mu^-)$. We show its marginalised distribution after dropping the lower likelihood penalties on $\Omega_{DM}h^2$ from the MCMC algorithm procedure in Fig. 9 as the histogram marked "extra DM allowed". For the purpose of comparison, the default calculation where we assume all dark matter to be thermal neutralinos from Fig. 4c is also displayed, being marked "no extra DM allowed". Comparing the two distributions, we see a broader distribution due to the enhanced A^0-pole annihilation region when additional components are allowed in